A New Approach for Refractive Index Sensing Using Hybrid Plasmonic Waveguides

Hesham A. Okda[1,2] and Hossam Shalaby[1,2], *Senior Member, IEEE*
[1]*Egypt-Japan University of Science and Technology (E-JUST), Alexandria 21934, Egypt*
[2]*Faculty of Engineering, Alexandria University, Alexandria 21544, Egypt*
hesham@alexu.edu.eg, shalaby@ieee.org

ABSTRACT
In this paper, we provide a comprehensive investigation for modes optical characteristics versus layers' thicknesses in straight hybrid plasmonic waveguides. Furthermore, we demonstrate how to exploit these characteristics to introduce a new simple scheme for sensing variations in surrounding refractive index by measuring phase difference between the TM and TE modes. The results show sensing sensitivity of 280° per refractive index unit (RIU) for a gas refractive index sensor, with a very compact device length of 5 μm.
Keywords: hybrid plasmonic waveguides, optical sensing.

1. INTRODUCTION

Recently, on-chip optical sensing has been one of the most relevant applications of hybrid plasmonic waveguides (HPWGs). This is because of the simultaneously achievable high confinement of optical power in sensing region, besides the relatively low propagation loss, compared with plasmonic-based sensors. However, most of the recently proposed structures for sensing surrounding refractive index variations are based on monitoring a resonance wavelength at which two propagating modes are being coupled, either through a grating structure [1], or by coupling between a photonic waveguide and a hybrid plasmonic ring resonator [2]. Accordingly, this increases sensor design complexity, as well as its footprint.

In this paper, we present a detailed investigation, supported with physical explanations, for the impacts of changing HPWG layers thicknesses on modal properties of the fundamental TM and TE modes. Furthermore, based on the obtained properties, we propose an alternative simple approach to detect surrounding refractive index changes using two straight HPWGs and a differential phase detector.

2. CHARACTERIZATION

Figure 1 illustrates a schematic diagram of the device to be investigated. It consists of two identical slab HPWGs injected with the fundamental TM and TE modes. The two modes propagate along the waveguides for a length L, before reaching a differential phase detector to measure the relative phase difference between them.

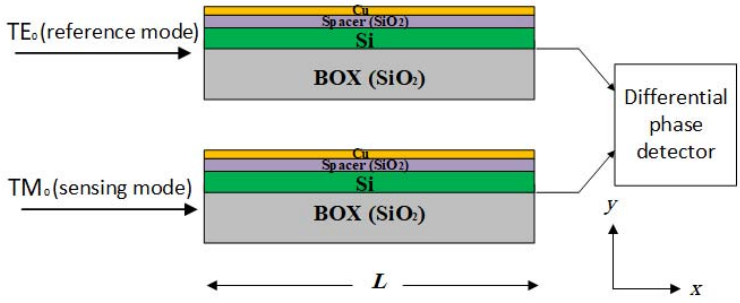

Figure 1. Schematic diagram of investigated device.

The general idea is to design the two waveguides with suitable dimensions, so as to achieve phase matching between the two modes when the surrounding medium is unperturbed. Accordingly, the phase difference in this case is zero, as the two modes would have the same propagation constant. Otherwise, if the surrounding refractive index, n_s, changed, the TM mode would be highly affected, and its effective index, n_{eff}, changes. Indeed, it can be employed as a sensing mode. In contrast, the TE mode has a negligible change in its n_{eff}, and subsequently it can be used as a reference mode. Hence, by relating the measured phase difference between the two modes to the changes in surrounding refractive index, the function of the new sensor is met.

Aside from its simple structure, another unique property of this kind of sensors is that its sensitivity can be tuned by adjusting waveguides length, L, which is linearly proportional to the phase shift, $\Delta\phi$, through the relation:

$$\Delta\varphi_m = \frac{2\pi}{\lambda}\cdot\left(\frac{\partial n_{eff}^m}{\partial n_s}\right)\cdot\Delta n_s\cdot L\,, \tag{1}$$

where λ is the operating wavelength, $\partial n_{eff} / \partial n_s$ represents mode effective index sensitivity, and m denotes TM or TE.

Although increasing L achieves higher sensitivity, it comes at the expense of more propagation loss. Hence, a high-power laser source is needed to guarantee sufficient signal power at the differential phase detector input.

In this context, it is worth noticing the important role of the differential phase detector in determining the minimal level of detection and the dynamic range of the proposed sensor. Differential phase detectors utilizing photonic crystals have been reported in [3,4]. However, introducing such a new type of sensors may motivate further research to achieve better accuracy and sensitivity for on-chip optical phase difference detection.

We employed the transfer matrix method (TMM) and MATLAB software to construct the modal dispersion relations of TM and TE modes, and subsequently to obtain the complex propagation constants, propagation lengths, as well as optical power distributions of the two modes in the proposed multilayer structure. In all our calculations, the total propagating power, along the x-direction, of each mode is normalized to 1 W.

3. RESULTS AND DISCUSSIONS

Considering the two waveguides shown in Fig. 1, and assuming an operating wavelength of 1550 nm, the refractive indices of silicon layer, spacer, and the upper copper film are obtained using Drude model to be 3.48, 1.444, and 0.19+j10.95 respectively. Here, we study device characteristics assuming surrounding air with unity refractive index.

Generally, there are three parameters to be investigated; namely, silicon thickness, t_1, spacer thickness, t_2, and copper film thickness, t_3. The effects of changing values of these parameters on the fundamental TM/TE modes are investigated and explained physically in detail. The optimization of the introduced sensor is performed by controlling these thicknesses to achieve the best performance.

3.1 Effect of Silicon Thickness on Evanescent Power

In Fig. 2, the evanescent power of the TM and the TE modes are obtained, and plotted versus silicon thickness, t_1. For the sake of simulation, t_2 and t_3 are set at 80 nm and 5 nm, respectively.

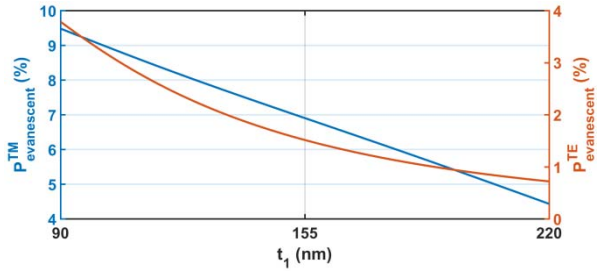

Figure 2. Percentage evanescent power of both TM and TE modes versus silicon thickness.

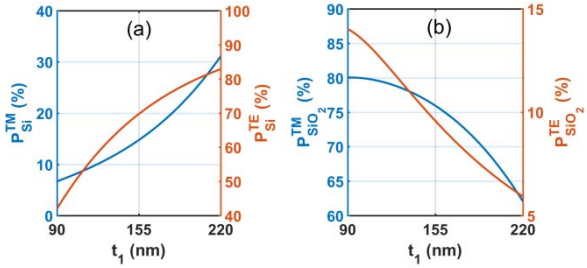

Figure 3. Percentage propagating power of both TM and TE modes in: (a) silicon; (b) silica spacer.

It is evident that increasing t_1 is associated with a decrease in the evanescent power leaking into ambient, for the two modes. That is because both modes have more guided optical power in thicker silicon layers, as revealed in Fig. 3(a) that illustrates the percentage propagating power guided in silicon for each mode.

In addition, an insight onto Fig. 2 reveals that, by increasing t_1, the evanescent power of the TE mode drops to low levels, while the TM mode still maintains higher power levels (nearly sixfold). This is attributed to the higher concentration of the TE mode power inside the silicon layer, compared with the TM mode which is mainly confined in the lower-index spacer, as revealed in Figs. 3(a) and 3(b) showing the percentage propagating power of each mode in silicon and silica spacer, respectively.

Now, the previously illustrated polarization spatial diversity of the fundamental TM and TE modes in HPWGs is exploited to optimize the performance of the proposed sensor by minimizing the sensitivity of the TE mode to refractive index changes in the surrounding medium. That is, by making silicon layer as thick as possible to suppress its evanescent power from leaking into ambient. Here, we choose t_1 = 220 nm, which is the maximal thickness of silicon layer typically provided by SOI standard.

3.2 Effect of Copper Film Thickness on Evanescent Power

In this subsection, the influence of the copper film thickness, t_3, on the modal characteristics of the fundamental TM and TE modes is investigated. Accordingly, these characteristics can be exploited to achieve further design optimization of the proposed sensor.

First, the evanescent power of each mode under test is calculated, for different values of t_3, and is plotted in Fig. 4, where t_1 and t_3 are adjusted at 220 nm and 80 nm, respectively. It is worth noticing that we start our simulation at t_3 = 5 nm because it has been found experimentally that this is the minimal thickness at which a copper film can be grown continuously [5].

It is found that, when thicker films are used, less optical power would leak into the surrounding ambient. Physically, this is due to the rising electromagnetic power dissipation in the copper film, as being an imperfect conducting medium. Obviously, the thicker the copper film is, the more is the decay of optical power inside it, and subsequently less optical power penetrates the surrounding ambient. Moreover, it is evident that, for very thin copper films, the evanescent power of the TM mode is noticeably much higher than that of the TE mode, which remains below 0.5% of the total mode power. This high observed dissimilarity of the evanescent power levels of the two modes is arising from the polarization spatial diversity property that is clarified above. Accordingly, with very thin copper films in the proposed sensor, one can expect promising performance because the TM will be highly sensitive to small changes in ambient refractive index, whereas the TE mode can be used as a reference mode that is almost not affected by those changes. Here, we choose the minimal copper film thickness (5 nm) for continuous growth, as mentioned above.

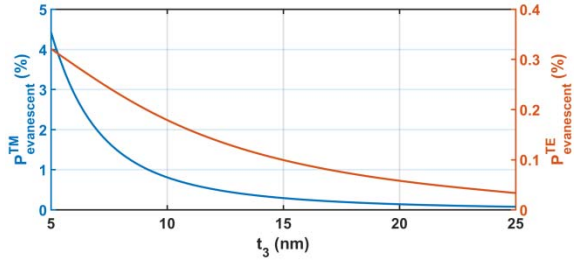

Figure 4. Percentage evanescent power of both TM and TE modes versus copper film thickness.

3.3 Effect of Spacer Thickness on Mode Effective Index and Propagation Loss

Now, the effect of changing spacer thickness, t_2, on both mode effective index, n_{eff}, and propagation loss, α, is explored. By the end of this subsection, the design of our proposed sensor is accomplished after choosing an appropriate value for t_2.

First, n_{eff} and α are obtained for the TM and TE modes, respectively, and plotted, in Fig. 6, versus t_2. Here, t_1 and t_3 are set to 220 nm and 5 nm, as obtained above.

Figure 5(a) reveals that the TM mode suffers from gradual drop in its effective index, as well as the associative propagation loss, with increasing t_2. This behaviour can be explained as follows. As being a hybrid mode, the TM mode alters from being plasmonic-like to be photonic-like, with increasing t_2, and the most of optical power of that mode is spread mainly within the low-index spacer, instead of being strongly confined just at the copper film. Accordingly, this process normally contributes to reducing the TM mode effective index and its propagation loss, as being less bound to the copper film.

On the other hand, for the TE mode, the electromagnetic boundary conditions imply that its optical power is pushed away from the copper film towards silicon. Accordingly, increasing spacer thickness boosts the refractive index above silicon layer, causing the effective index of the TE mode to be higher, as evident from Fig. 5(b). Meanwhile, the existence of a thicker spacer provides more separation between optical power of the TE mode and the copper film. As a result, the propagation loss of the TE mode declines with increasing t_2, as Fig. 5(b) reveals, because it is being less affected by the copper film.

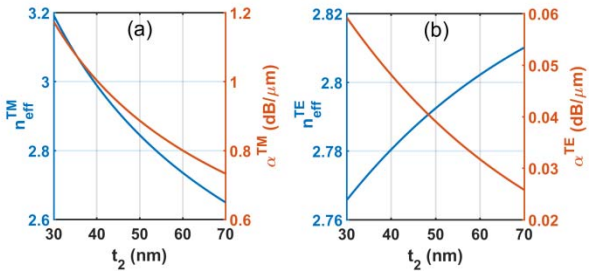

Figure 5. Effective index and propagation loss of: (a) TM mode; (b) TE mode versus spacer thickness.

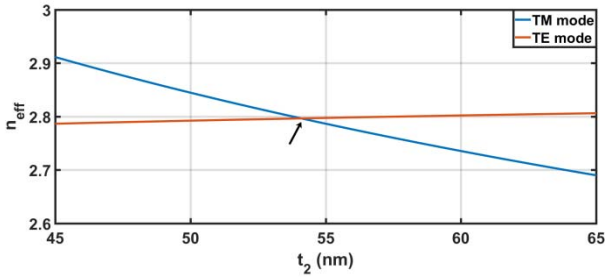

Figure 6. Phase matching of TM and TE modes.

At this point, we are to employ the illustrated behaviour dissimilarity of TM and TE modes to choose spacer thickness for the proposed sensor according to the following criterion. With no perturbation in the surrounding refractive index, zero phase difference should be observed between the TM and TE modes at the phase detector. The above rigorous condition implies that the two modes should be matched in phase if the surrounding medium is air (n_s = 1). In Fig. 6, we plot n_{eff} of the two modes, on the same vertical axis, versus t_2.

It is evident that the intersection point occurs at t_2 = 54 nm, which leads to perfect phase matching between the two modes. Turning to Fig. 5(a), we obtain the corresponding propagation loss of the TM mode as 0.82dB/μm, from which we can directly calculate the propagation length to be around 5 μm.

3.4 Evaluating Sensor Performance

Having determined the proper values for t_1, t_2, and t_3, the sensitivity of the TM and the TE modes is examined now by introducing a small perturbation to the surrounding refractive index, n_s, and calculating the first derivative of n_{eff} with respect to n_s, for each mode. To do that, the TM and TE modal dispersion relations are constructed, using TMM, and then solved analytically, using MATLAB, for a small range of n_s. Next, the quantity $\partial n_{eff}/\partial n_s$ is obtained numerically, for the two modes, and is plotted in Fig. 7.

It is strikingly obvious, from Fig. 7, that, whereas the TE mode exhibits nearly zero sensitivity to surrounding refractive index variations, the TM mode, on the other hand, is significantly affected by even small variations of n_s. Accordingly, the principal design condition introduced in Sec. 2 is met, where the TE mode can be used as a reference mode, while the shift in the effective index value of the TM mode reflects the changes in surrounding refractive index.

Now, the sensitivity of the proposed sensor can be estimated by employing modes sensitivities obtained from Fig. 7 in Eq. (1) to directly link the incremental changes in surrounding refractive index, Δn_s, with the net phase difference, $\Delta\Phi_{net}$, between the two device arms. Figure 8 illustrates the calculated phase angles of TM and TE modes at the output, besides to their difference, assuming that the device length equals the propagation length of the TM mode, which is calculated above to be 5 μm.

Interestingly, Fig. 8 reveals that the net phase difference almost equals the phase variations of the TM mode that increases linearly with Δn_s, whereas the reference TE mode shows a negligible phase variation for various Δn_s values. One can estimate the sensitivity of the proposed phase-difference-based sensor to be about 280°/RIU.

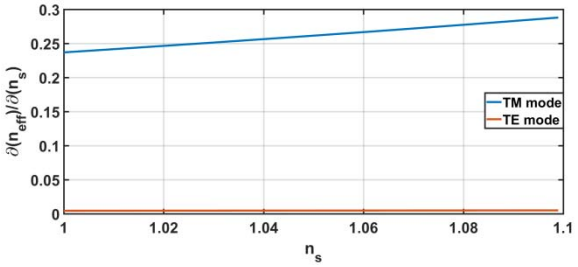

Figure 7. Sensitivity of TM and TE modes versus surrounding refractive index.

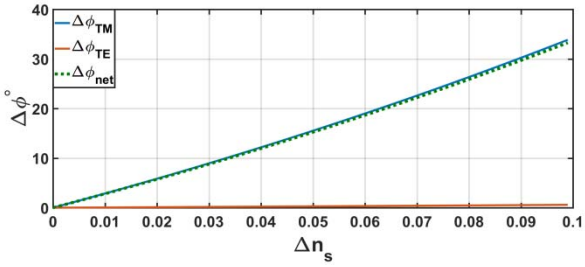

Figure 8. Phase variations and net phase difference versus changes in surrounding refractive index.

4. CONCLUSIONS

We demonstrated a new scheme of surrounding refractive index sensors based on detecting phase difference between the fundamental TM and TE modes in two identical straight hybrid plasmonic waveguides. A rigorous analysis was performed to determine an appropriate thickness for each layer of the waveguides that leads to optimized performance of the proposed phase-difference-based sensor. Silicon layer was set to be as thick as 220 nm to minimize the reference TE mode sensitivity to surrounding refractive index variations, while copper film thickness was minimized at 5 nm to increase sensitivity of the TM mode. On the other hand, spacer thickness was determined to be 54 μm to achieve phase matching between the two modes when the surrounding is unperturbed. Our results showed sensor sensitivity of 280°/RIU, when the surrounding is air, with a compact length of 5 μm.

ACKNOWLEDGEMENTS

This work is financially supported by the Ministry of Higher Education, Egypt (MoHE).

REFERENCES

[1] P. Kaur and M. R. Shenoy: Highly sensitive refractive index sensor based on silicon nitride strip waveguide directional coupler, *Sensors Letters*, vol. 2, pp. 1-4, Jan. 2018.

[2] M. A. Butt, S. N. Khonina, and N. L. Kazanskiy: Highly sensitive refractive index sensor based on hybrid plasmonic waveguide microring resonator, *Waves in Random and Complex Media*, pp. 1-8, Aug. 2018.

[3] V. S. Amaratunga *et al.*: Photonic crystal phase detector, *J. Opt. Soc. Am. B*, vol. 25, pp. 1532-1536, Sep. 2008.

[4] M. Danaie, and H. Kaatuzian: Design of a photonic crystal differential phase comparator for a Mach-Zehnder switch, *J. Opt.*, vol. 13, pp. 1-6, Dec. 2010.

[5] A. A. Solovyev *et al.*: Properties of ultra-thin Cu films grown by high power pulsed magnetron sputtering, *Thin Solid Films*, vol. 631, pp. 72-79, Jun. 2017.